Journal of Thrombosis and Haemostasis, **6**: 837–845 DOI: 10.1111/j.1538-7836.2008.02937.x

ORIGINAL ARTICLE

Thrombostatin FM compounds: direct thrombin inhibitors – mechanism of action *in vitro* and *in vivo*

M. T. NIEMAN,* F. BURKE,† M. WARNOCK,‡ Y. ZHOU,* J. SWEIGART,* A. CHEN,* D. RICKETTS,* B. R. LUCCHESI,§ Z. CHEN,¶ E. DI CERA,¶ J. HILFINGER,** J. S. KIM,** H. I. MOSBERG† and A. H. SCHMAIER*

**Division of Hematology and Oncology, Department of Medicine, Case Western Reserve University, Cleveland, OH; †College of Pharmacy; ‡Department of Medicine; §Department of Pharmacology, University of Michigan, Ann Arbor, MI; ¶Department of Biochemistry and Molecular Biophysics, Washington University School of Medicine, St Louis, MO; and **TSRL Inc., Ann Arbor, MI, USA*

To cite this article: Nieman MT, Burke F, Warnock M, Zhou Y, Sweigart J, Chen A, Ricketts D, Lucchesi BR, Chen Z, Di Cera E, Hilfinger J, Kim JS, Mosberg HI, Schmaier AH. Thrombostatin FM compounds: direct thrombin inhibitors – mechanism of action *in vitro* and *in vivo*. *J Thromb Haemost* 2008; **6**: 837–45.

Summary. *Background:* Novel pentapeptides called Thrombostatin FM compounds consisting mostly of D-isomers and unusual amino acids were prepared based upon the stable angiotensin converting enzyme breakdown product of bradykinin – RPPGF. *Methods and Results:* These peptides are direct thrombin inhibitors prolonging the thrombin clotting time, activated partial thromboplastin time, and prothrombin time at ≥0.78, 1.6, and 1.6 μM, respectively. They competitively inhibit α-thrombin-induced cleavage of a chromogenic substrate at 4.4–8.2 μM. They do not significantly inhibit plasma kallikrein, factor (F) XIIa, FXIa, FIXa, FVIIa-TF, FXa, plasmin or cathepsin G. One form, FM19 [rOicPaF(*p*-Me)], blocks α-thrombin-induced calcium flux in fibroblasts with an IC_{50} of 6.9 ± 1.2 μM. FM19 achieved 100% inhibition of threshold α- or γ-thrombin-induced platelet aggregation at 8.4 ± 4.7 μM and 16 ± 4 μM, respectively. The crystal structure of thrombin in complex with FM19 shows that the N-terminal D-Arg retrobinds into the S1 pocket, its second residue Oic interacts with His-57, Tyr-60a and Trp-60d, and its C-terminal *p*-methyl Phe engages thrombin's aryl binding site composed of Ile-174, Trp-215, and Leu-99. When administered intraperitoneal, intraduodenal, or orally to mice, FM19 prolongs thrombin clotting times and delays carotid artery thrombosis. *Conclusion:* FM19, a low affinity reversible direct thrombin inhibitor, might be useful as an add-on agent to address an unmet need in platelet inhibition in acute coronary syndromes in diabetics and others who with all current antiplatelet therapy still have reactive platelets.

Correspondence: Alvin H. Schmaier, Division of Hematology and Oncology, Department of Medicine, Case Western Reserve University, 10900 Euclid Avenue, WRB2-130, Cleveland, OH 44106-7284, USA.
Tel.: +1 216 368 1172; fax: +1 216 368 3014.
E-mail: schmaier@case.edu

Received 13 January 2008, accepted 19 February 2008

Keywords: bradykinin, thrombin, thrombin inhibitor, thrombostatin, platelets, RPPGF.

Introduction

Oral antiplatelet therapy has become the mainstay of pharmacologic treatment for the prevention of adverse thrombotic cardiovascular events. Aspirin and clopidogrel are the currently available oral antiplatelet agents [1]. Growing evidence indicates that reduced responsiveness to the current antiplatelet agents is associated with adverse clinical coronary artery events [2]. In diabetic patients, a quartile can be found who even with aspirin and clopidogrel therapy have highly reactive platelets that are predictive of future coronary events [3]. Alternatively, more potent P2Y12 antagonists reduce coronary events with the trade-off of increased significant bleeding summating in no improvement in overall outcome [4]. Thus, additional antiplatelet agents are needed that provide novel mechanisms for platelet inhibition with reduced bleeding risk.

The angiotensin-converting enzyme (ACE) breakdown product of bradykinin, RPPGF, inhibits thrombin-induced platelet aggregation, inhibits protease activated receptor 1 and 4 (PAR1 and PAR4) mediated calcium mobilization, prolongs clotting assays, prolongs the time for thrombosis in mouse carotid injury models, and when infused in man inhibits thrombin-induced platelet activation [5–9]. Using RPPGF as a model sequence, studies substituted natural amino acids with D-isomers and/or unusual amino acids to make compounds more potent and resistant to degradation in biologic fluids. TH146 (rOicPGF) was the first generation change with a D-arginine and an Oic in residues 1 and 2 of the sequence, respectively [7]. It is 4- to 5-fold more potent than RPPGF [7]. Additional studies increased the potency and *in vivo* stability of TH146 by substitutions of the fourth and fifth amino acid residues of the sequence (Table 1) [10]. The present investigations describe the mechanism of action, *in vivo* effect, and oral availability of the compounds, called Thrombostatin™ 'FM', with these latter modifications.

Table 1 Influence of FM compounds on thrombin-induced platelet aggregation and calcium mobilization

Peptide	Sequence	Platelet aggregation minimal concentration for 100% inhibition (μM)*	Calcium mobilization (% inhibition at 5 μM)†
RPPGF‡	RPPGF	680 ± 280	–
TH146§	rOicPGF	140 ± 20	–
FM19	rOicPaF(*p*-Me)	16 ± 4	69
FM29	rOicPsF(*p*-Me)	16 ± 4	56
FM33	rOicPaF(*p*-Br)	18 ± 4	35
FM36	rOicPaF(*p*-I)	23 ± 3	36
FM39	rOicPaF(*p*-NO_2)	33 ± 8	26
FM43	F(*p*-Me)OicrPa	>1000	NI¶
FM44	aPrOicF(*p*-Me)	>1000	NI¶
FM45	PaF(*p*-Me)rOic	> 1000	NI¶
FM46	PF(*p*-Me)Oicra	150 ± 70	NI¶
FM47	PraF(*p*-Me)Oic	>1000	NI¶
FM48	PrOicF(*p*-Me)a	>1000	NI¶

*The minimal concentration for 100% inhibition of γ-thrombin induced platelet aggregation ± SEM, $n > 3$. †The percent inhibition of α-thrombin-induced calcium mobilization at 5 μM peptide. ‡From Hasan *et al*. [6]. §From Nieman *et al*. [7]. ¶No inhibition (NI) of α-thrombin-induced calcium mobilization of 20 μM peptide.

Materials and methods

Peptides and reagents

Standard single letter abbreviations are used for L-amino acids and lowercase letters are used to designate D-amino acids. The synthetic amino acid (2S, 3aS, 7aS)-octahydroindol-2-carboxlic acid is abbreviated (Oic). Peptides Arg-Pro-Pro-Gly-Phe (RPPGF) and D-Arg-Oic-Pro-Gly-Phe (rOicPGF or TH146) were synthesized by Multiple Peptide Systems, Inc., San Diego, CA, USA (Table 1). The FM series of compounds (Table 1) were prepared as previously described [10]. The structure of FM19 [rOicPaF(*p*-Me)] is shown in Fig. 1. All peptides used in these studies were greater than 95% pure and characterized by analytical HPLC, amino acid analysis, and mass spectrometry. The peptides were colorless, odorless, and soluble in water.

Platelet aggregation

Each peptide was screened for its ability to inhibit γ-thrombin-induced platelet aggregation. Fresh whole blood was used to prepare platelet-rich plasma (PRP) and platelet aggregation studies were performed as previously reported [7]. PRP was treated with variable concentrations of γ-thrombin (3000 U mg^{-1}, Haematologic Technologies, Essex Junction, VT, USA) to determine the minimal or threshold concentration for platelet aggregation. γ-Thrombin was used as the platelet agonist, as it does not proteolyze fibrinogen to form a fibrin clot. The minimal concentration of each peptide to achieve 100% inhibition of threshold platelet aggregation was determined. In other experiments, platelets in PRP were washed by gel filtration in HEPES-Tyrode's buffer and the minimal concentration of FM19 and FM29 that inhibited threshold human α-thrombin-induced (3000–3250 U mg^{-1}, Haematologic Technologies) platelet aggregation was determined [7].

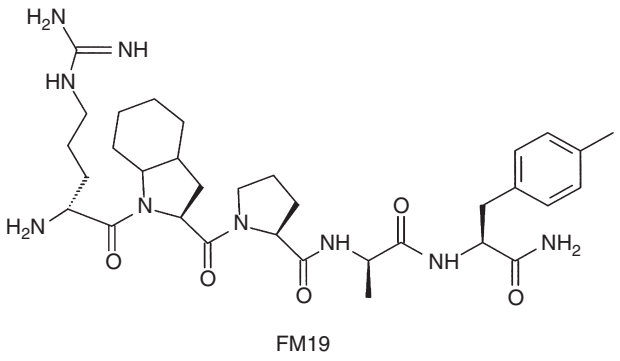

FM19

Fig. 1. The structure of FM19, rOicPaF(*p*-Me)–NH_2.

Calcium mobilization

Each peptide was assayed for its ability to inhibit α-thrombin-induced calcium mobilization in normal human lung fibroblasts, as previously reported [6,7]. The degree of inhibition of α-thrombin-induced Ca^{2+} flux for each peptide was determined by calculating the area under the curve by Winlab software (Perkin Elmer, Torrence, CA, USA) and is expressed as percent activity; samples without peptide (thrombin alone) were set to 100%.

Coagulation assays

The effect of FM19, FM29, FM33, or FM36 on the activated partial thromboplastin time (APTT), prothrombin time (PT), or thrombin clotting time (TCT) was determined as previously described [6,7].

Inhibition of enzyme cleavage of chromogenic substrates

Inhibition of chromogenic activity of α-thrombin, was determined by adding α-thrombin (0.5 nM) to 2–100 μM

H-D-Phe-Pip-Arg-pNA (S2238) in the presence or absence of FM compounds (3–30 μM) in 10 mM Tris-HCl and 150 mM NaCl pH 8.0. Absorbance data for kinetic assays were collected using a microplatelet reader (NOVAstar, BMG Labtech, Offenburg, Germany; or Wallac Victor^3 1420 Multilabel Counter, PerkinElmer Life and Analytical Sciences, Boston, MA, USA) and progress curves were plotted in Microsoft Excel. Models of inhibition were determined according to the Akaike Information Criteria (AIC) as calculated in SigmaPlot (Systat Inc.) [11]. Additional studies determined the influence of 100–1000 μM FM19 on other coagulation proteases. Inhibition of factor (F) VIIa (Haematological Technologies) in a preformed complex with soluble recombinant tissue factor, amino acids 1–219 ($sTF_{1\text{-}219}$), provided by Dr Tom Girard (Monsanto, St Louis, MO, USA), and inhibition of human FXa and FXIa (Haematological Technologies) were performed as previously described [7]. Inhibition studies of plasma kallikrein or FXIIa (Enzyme Research Laboratories, Inc., South Bend, IN, USA) used 0.1–2 mM H-D-Pro-Phe-Arg-*p*-nitroanalide (S2302) (Diapharma Chromogenix, Milano, Italy) in 50 mM Tris-HCl and 150 mM NaCl, pH 8.0. Inhibition of Cathepsin G (Calbiochem) was determined with 0.36–4.5 mM Suc-AAPF-*p*-nitroanalide (Calbiochem) in 100 mM Tris-HCl and 500 mM NaCl in 10% DMSO, pH 7.4. Inhibition of plasmin (Haematological Technologies) was determined with 0.1–2 mM H-D-valyl-L-leucyl-L-lysine-*p*-nitroanilide (S2251) in 10 mM Tris-HCl and 150 mM NaCl pH 8.0.

Crystallization of the thrombin-FM19 complex

Crystals of the complex of human thrombin R77aA and inhibitor FM19 were grown by the hanging drop vapor-diffusion method. The mutation R77aA abolishes the site of autoproteolysis and confers improved stability to thrombin for crystallization in the free form, or in complex with weak active site inhibitors [12]. A solution of R77aA (5 mg mL^{-1} in 2 μL) in 50 mM choline chloride, 20 mM Tris, pH 7.4 was mixed with an equal volume reservoir solution containing 20% PEG 3350, 100 mM Bis-Tris, pH 7.5 and 200 mM NaI, and left to equilibrate at 23 °C. Single crystals grew to an approximate size of 0.45 × 0.15 × 0.1 μL in one to two weeks. Crystals were hexagonal, space group $P6_122$, with unit cell parameters $a = b = 80.9$ Å, $c = 183.7$ Å, and contained one molecule per asymmetric unit. X-ray data were collected to 1.8 Å resolution from a crystal soaked in Paraffin oil (Hampton Research, Aliso Viejo, CA, USA) for 5 min at 100°K on an ADSC Quantum-315 CCD detector at the Biocars Beamline 14-BM-C of the Advanced Photon Source, Argonne National Laboratories, Argonne, IL, USA. Data processing including indexing, integrating, and scaling was performed using the HKL2000 package [13]. The structure was solved by molecular replacement with MOLREP from the CCP4 package [14] using the coordinates of the PPACK-inhibited form of human thrombin R77aA [Protein Data Bank (PDB) ID code 1SFQ] [12] as a starting model, with inhibitors, sugars, and solvent molecules omitted as the starting model. Refinement and electron density generation were performed with the Crystallography and NMR System software package [15] and 5% of the reflections were randomly selected as a test set for cross validation. Ramachandran plots were calculated using PROCHECK [16]. Results of data collection, processing, and refinement are listed in Table 4. Coordinates of the structure of the human thrombin–FM19 complex have been deposited to the PDB (PDB ID code 3BV9).

Pharmacokinetic and metabolic studies

Purpose-bred beagle dogs (9–11 kg) were prepared for the pharmacokinetics studies as previously reported [7]. After a single intravenous administration of FM19 (4.4 mg kg^{-1} in 5 mL saline infused over 1 min into each of four different dogs), blood samples were collected at 1, 5, 10, 15, 20, 25, 30, 40, 60, 90, and 120 min by withdrawing 5 mL blood into a syringe containing 3.8 g% sodium citrate (1:9, citrate:blood) to prepare platelet-poor plasma that was stored in small aliquots at −70 °C until assay [7]. Similarly, five male and five female Sprague–Dawley rats were injected with 17 mg kg^{-1} FM19 in a dose volume of 5 mL kg^{-1} over 5 min and samples were collected for analysis. The pharmacokinetic characteristics were calculated using non-compartmental methods of Rowland and Tozer [17]. FM19 in canine and rat plasma was assayed by liquid chromatography/mass spectroscopy/mass spectroscopy (LC/MS/MS) assay (see Supplementary material). The metabolic stability of FM19 in liver microsomes from human, canine, and rat hepatocytes was also performed (see Supplementary material).

Mouse thrombosis studies

Mice, 8–16 weeks of age, were prepared for carotid artery thrombosis studies using Rose Bengal (4, 5, 6, 7-tetrachloro-3′, 6-dihydroxy-2, 4, 5, 7-tetraiodospiro (isobenzofuran-1(3H), 9 [9H] xanthan)-3-1 dipotassium salt) (Fisher Scientific, Fair Lawn, NJ, USA) as previously reported [7]. Thrombosis experiments were performed using three different routes of FM19 administration: intraperitoneal (IP) injections, intraduodenal installation, and oral administration in drinking water. In initial investigations, FM19 was given between 0.2 and 3.22 mg kg^{-1} IP. In other experiments, a celiotomy was performed and after isolation of the proximal duodenum, FM19 was instilled by intraluminal injection at 8.25, 16.5, or 33 mg kg^{-1} using 25 gauge needle injections. Plasma samples were collected for coagulation studies and other animals were examined on the thrombosis assay. Experiments also were performed in mice by adding FM19 (3, 5, or 10 mg mL^{-1}) to the drinking water. After two to seven days, the mice were examined for their time to thrombosis (Rose Bengal) assay and plasmas were used to determine FM19 levels by LC/MS/MS assay while plasmas from other treated animals was sampled for FM19's influence on the TCT assay.

Statistical analysis

Comparison between groups was made by the Student's *t*-test using non-paired data with a non-parametric analysis (Prism, Graphpad Software Inc., San Diego, CA, USA). Significance is defined as a *P*-value < 0.05.

Results

Initial investigations determined which of the rOicPGF analogs with substitutions at residues 4 and 5 were most potent inhibitors of γ-thrombin-induced platelet aggregation in PRP (Table 1) [7]. The minimal concentration of peptide required for 100% inhibition of threshold γ-thrombin-induced platelet aggregation was determined and compared to RPPGF and TH146. The top five peptides were 4- to 9-fold more potent than TH146 and twenty- to forty-threefold more potent than RPPGF (Table 1). Two peptides, FM19 and FM29, were chosen for further study. Five scrambled analogs of FM19 [rOicPa(*p*-Me)], FM43, FM44, FM45, FM47, and FM48, each containing the same amino acids as FM19, but in a different sequence, did not inhibit γ-thrombin-induced platelet aggregation at 1000 μM (Table 1). A sixth scrambled analog, FM46, did inhibit γ-thrombin-induced platelet aggregation at 150 μM; however, this potency is ~tenfold lower than that of FM19. When using gel-filtered human platelets, FM19 and FM29 were found to inhibit threshold (~2 nM) α-thrombin-induced platelet aggregation 100% at 8.4 ± 4.7 μM and 11 ± 2.9 μM (mean ± SEM, $n = 5$), respectively.

Investigations next determined the ability of these peptides to inhibit α-thrombin-induced calcium mobilization in normal human lung fibroblasts. Studies determined the percent inhibition at 5 μM for each peptide (Table 1). The most potent inhibitors of calcium mobilization were FM19 and FM29 with 69 and 56 percent inhibition, respectively. The percent inhibition for FM33, FM36, and FM 39 was 2- to 3-fold lower than FM19 (Table 1). Importantly, scrambled versions of FM19 (FM43–48) did not inhibit calcium mobilization at either 5 or 20 μM peptide (Table 1). FM19 and FM29 inhibited α-thrombin-induced Ca^{2+} flux with an IC_{50} of 6.9 ± 1.2 and 5.4 ± 1.9 μM, respectively ($P = 0.54$; Fig. 2). The IC_{50} of these peptides is nineteenfold lower than TH146 (130 ± 17 μM) [7].

Previous studies determined that both RPPGF and TH146 inhibit coagulation assays [6,7]. There was significant prolongation ($P < 0.05$) of the APTT at 1.6 and 3.1 μM for FM19 and FM29, respectively (Fig. 3A, Table 2). The APTT was less affected by FM33, FM36, and FM39. The PT was significantly prolonged at 1.6 μM for FM19 and FM29, but less influenced by FM33, FM36, and FM39 (Fig. 3B, Table 2). At 6.3 μM, FM29 and FM19 prolonged the APTT and PT 24–25% and 17–30%, respectively. In contrast, the TCT was significantly prolonged at 0.78 μM for each peptide with the exception of FM29, which was significant at 0.39 μM (Fig. 3C, Table 2). At 1.6 μM, FM29 and FM19 prolonged the TCT 33 and 45%, respectively. The latter data indicated that these compounds are direct thrombin inhibitors.

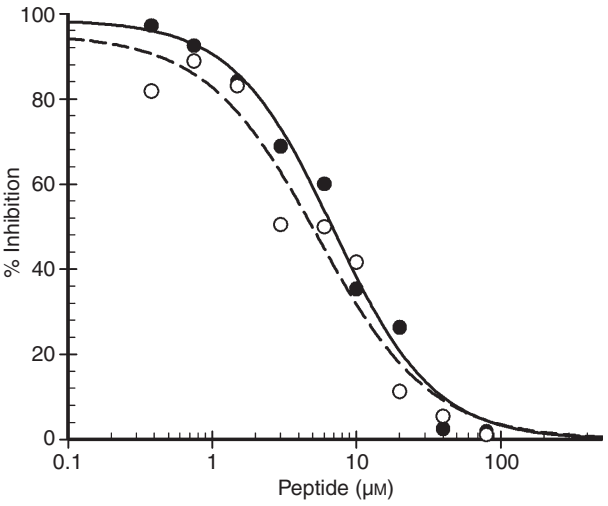

Fig. 2. Influence of FM19 and FM29 on α-thrombin-induced intracellular calcium mobilization. Normal lung fibroblasts were loaded with Fura-2 and incubated in the absence or presence of FM19 (●) or FM29 (○). After incubation, cells were treated with the minimal concentration of human α-thrombin that induces calcium mobilization. Values for each concentration of peptide were determined by calculating the area under the curve and are expressed as percentage of calcium flux. Samples with no peptide inhibitor were set to 100%. The data represent the mean ± SD of at least three experiments. The best fit was determined by a four parameter logistical function.

Since bradykinin, RPPGF, and TH146 ($K_i = 97$ μM) bind directly to the active site of thrombin to interfere with its enzymatic activity [6,7,18], investigations determined the concentration of the FM compounds required to inhibit α-thrombin. FM19 was a direct competitive inhibitor of α-thrombin with a K_i of 4.4 ± 2.4 μM (Fig. 4, Table 3). Similarly, FM29, FM33, FM36, and FM39 were also competitive inhibitors of α-thrombin with a K_i of 5.1 ± 2.6, 8.2 ± 3.3, 4.1 ± 1.3, and 9.8 ± 3.8 μM, respectively (mean ± 95% confidence interval, Table 3). The data were fit to eight models of enzyme inhibition based on a global analysis. The best fits were chosen by the AIC, as previously described [11]. In each case, the data clearly fit to a competitive model. These data are supported by crystallography (Fig. 5). Although each peptide inhibited thrombin's enzymatic activity to a similar degree, FM19 was chosen for further investigation because it was the most active compound across most assays. On enzymatic assays unique for each enzyme, FM19 did not inhibit FXIIa, FVIIa-TF, FIXa, FXIa, plasma kallikrein, plasmin or cathepsin G at 1.0 mM (data not shown). FM19 inhibited FXa with a K_i of 510 μM. Therefore, FM19 is a relatively specific inhibitor of α-thrombin that has a twentyfold more potent K_i than TH146 [7].

Crystallography

Human thrombin carrying the single Ala substitution of Arg-77a in exosite I was crystallized in complex with FM19 at a resolution of 1.8 Å. The overall structure is similar to that of

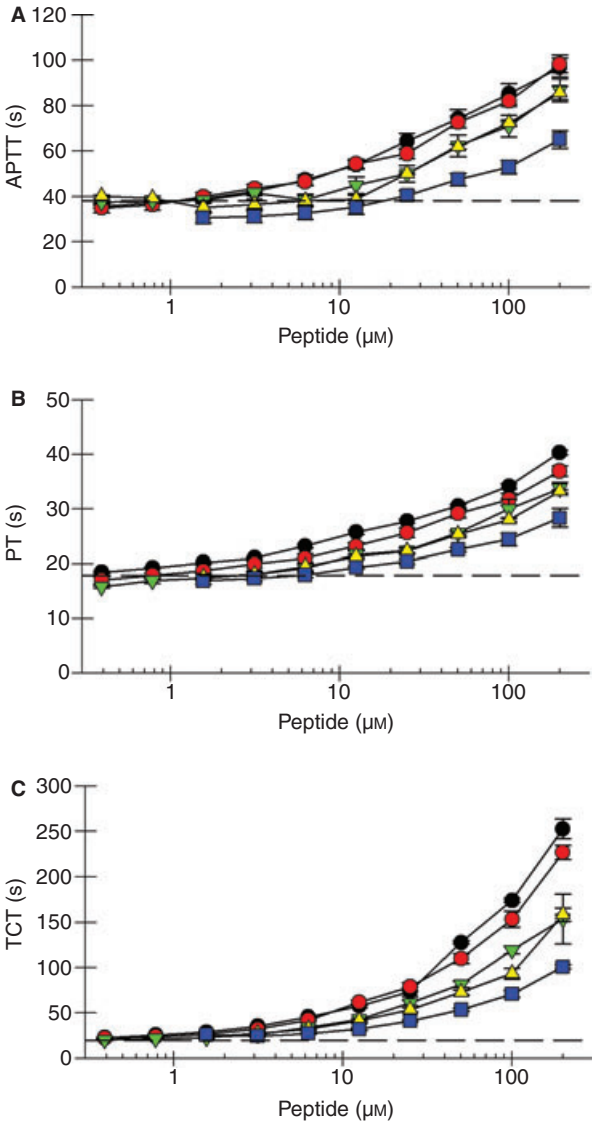

Fig. 3. Influence of FM compounds on coagulation assays. Normal human plasma was incubated with FM19 (●), FM29 (●), FM33 (▲), FM36 (▼) or FM 39 (■) and the activated partial thromboplastin time (A), prothrombin time (B), and thrombin clotting time (C) were determined as described in Materials and Methods. The data represent the mean ± SD of at least three independent experiments. The horizontal dashed line represents the assay in the absence of peptide.

Table 2 Influence of FM compounds on clotting assays

	Minimal concentration (μM) for prolongation ($P < 0.05$)		
Peptide	APTT	PT	TCT
TH146*	31	62	7.8
FM19	1.6	1.6	0.78
FM29	3.1	1.6	0.39
FM33	12.5	6.3	0.78
FM36	25	6.3	0.78
FM39	50	6.3	0.78

*From Nieman *et al.* [7]. APTT, activated partial thromboplastin time; PT, prothrombin time; TCT, thrombin clotting time.

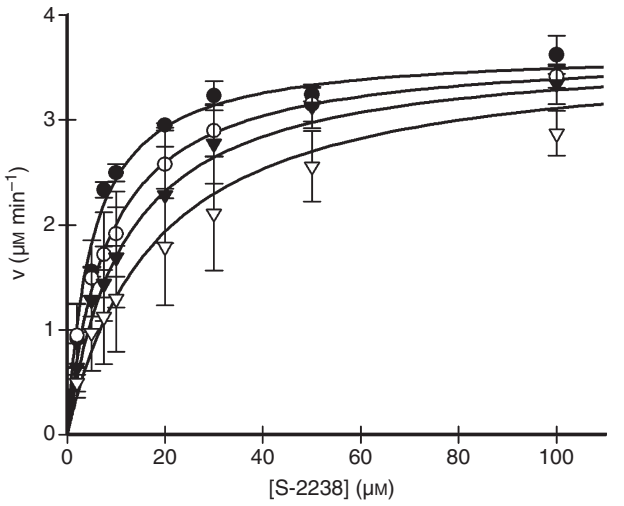

Fig. 4. α-Thrombin cleavage of S2238 in the absence or presence of FM19. α-Thrombin (0.5 nM) was added to S2238 (2–100 μM) in the absence (●) or presence of 3 (○), 6 (▼) or 12 (▽) μM FM19. Initial velocity data were fit to eight models of enzyme inhibition using a global analysis nonlinear least-squares analysis to determine the K_i and type of inhibition (see Methods). The data represent the mean ± SD of at least three independent experiments.

Table 3 Inhibition of α-thrombin induced cleavage of S2238 by FM compounds

Peptide	K_i (μM)†	Inhibition type
FM19	4.4 ± 2.4	C*
FM29	5.1 ± 2.6	C
FM33	8.2 ± 3.3	C
FM36	4.1 ± 1.3	C
FM39	7.5 ± 3.2	C

C, competitive inhibition. *In 10 mM Tris-HCl, 150 mM NaCl at pH 8.0 and 25 °C. †With a ± 95% confidence interval.

the PPACK-inhibited Na^+-bound form of thrombin [12], with a root-mean-squared deviation (rmsd) of only 0.325 Å (Table 4). The inhibitor penetrates the active site of the enzyme in the unusual retro-binding orientation (Figs. 5A and B) as first observed for the RPPGF peptide [6]. Notably, FM19 makes few polar contacts with thrombin, and the only direct interaction is mediated by H-D-Arg. The NH2 atom engages the Oδ2 atom of Asp-189 (2.83 Å), O atom of Gly-218 (3.05 Å), and O atom of Ala-190 (3.38 Å) in H-bonding interactions. The NH1 atom formed a H-bond to the Oδ1 atom of Asp-189 (3.00 Å). Finally, the N atom establishes a weaker H-bond with the O atom of Gly-219 favored by its flipped conformation in the enantiomeric D form. The rest of the polar interactions are mediated by four water molecules (w113, w59, w77, and w43) sandwiched between the inhibitor and the 216–219 β-strand of thrombin (Fig. 5B). Water w113 bridges the O terminal atom of FM19 (2.89 Å) and the Oε2 atom of Glu-217 (2.67 Å). Water w59 close by bridges the O terminal atom of FM19 (2.70 Å) and the N atom of Gly-219 (3.27 Å). Water w77 bridges the N atom of H-D-Ala of FM19 (2.95 Å) and the N atom of Gly-219 (3.48 Å). Finally, water w43 establishes another connection for the N atom of H-D-Arg of FM19

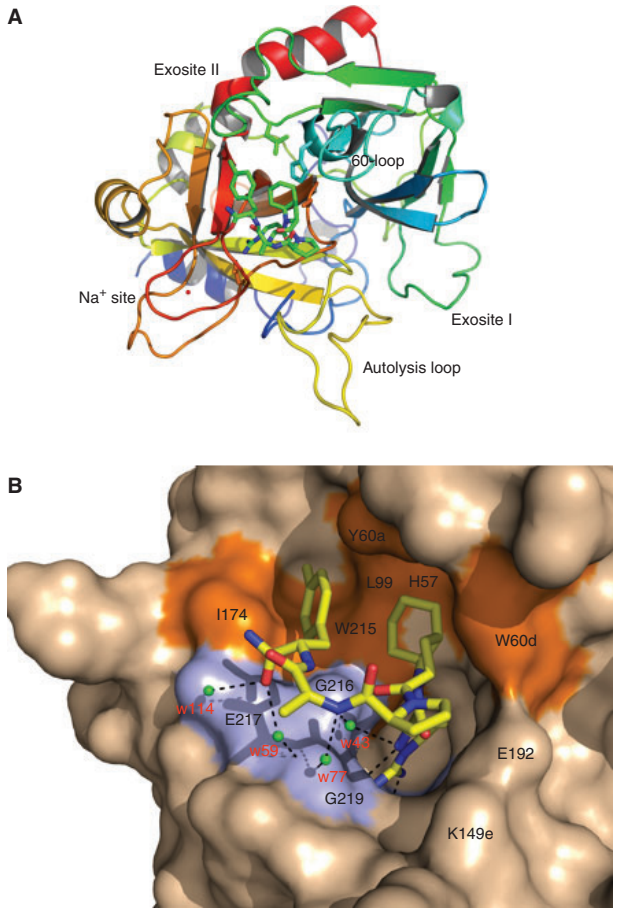

Fig. 5. Structure of the human thrombin mutant R77aA in complex with the inhibitor FM19. (A) Thrombin is rendered as a ribbon colored according to the spectrum (N-terminus blue, C-terminus red) and the bound FM19 is rendered in CPK with C atoms in green. Relevant regions of the enzyme are labeled. The bound Na^+ is in red and the side chains of Asp-189 in the primary specificity pocket and of residues of the catalytic triad (His-57, Asp-102, and Ser1-95) are shown as sticks. Note the integrity of the autolysis loop that is usually disordered in thombin structures. (B) Details of the molecular contacts at the thrombin–FM19 interface, with hydrophobic regions of the thrombin epitope colored in orange and polar regions colored in light blue. The thrombin surface is rendered in wheat and FM19 is in CPK model with C atoms in yellow. H-bonds are depicted as broken lines. Water molecules mediating contacts with the 216–219 β-strand of the enzyme are labeled in red.

(3.09 Å) with the O atom of Gly-216 (2.79 Å). These water-mediated interactions likely add specificity to binding and suggest ways to optimize FM19 further. The bulk of the binding epitope is provided by extensive hydrophobic interactions. The bicyclic side chain of Oic engaged in van der Waals interactions with the catalytic His-57, Tyr-60a, and Trp-60d, whose indole ring is shifted >4 Å relative to the position seen in the 1SFQ structure of thrombin [12]. The second Pro ring makes no contact with the enzyme, but causes the side chain of Glu-192 to relocate and establish a strong H-bond (2.88 Å) with the side chain of Lys-149e in the hinge region of the autolysis loop. This interaction is rarely observed in thrombin structures and has the unusual consequence of stabilizing the entire autolysis loop with additional strong H-bonds between

Table 4 Crystallographic data for human thrombin bound to FM19 (PDB ID 3BV9)

Data collection	
Wavelength (Å)	0.9
Space group	$P6_122$
Unit cell dimension (Å)	a = 80.9, b = 80.9, c = 183.7
Molecules/asymmetric unit	1
Resolution range (Å)	40.0–1.8
Observations	247 117
Unique observations	32 820
Completeness (%)	96.9 (87.6)
R_{sym} (%)	7.8 (24.1)
I/σ(I)	19.8 (3.2)
Refinement	
Resolution (Å)	40.0–1.8
|F|/σ(|F|)	>0
R_{cryst}, R_{free}	0.190, 0.239
Reflections (working/test)	31 172/1634
Protein atoms	2323
Solvent molecules	273
Inhibitor atoms	47
Glycerol/Na^+/I^-	2/1/3
Rmsd bond lengths* (Å)	0.012
Rmsd angles* (°)	1.7
Rmsd ΔB (Å^2) (mm/ms/ss)	3.40/3.99/5.46
<B> protein (Å^2)	26.8
<B> solvent (Å^2)	34.2
<B> glycerol/Na^+/I^- (Å^2)	52.8/22.5/29.7
Ramachandran plot	
Most favored (%)	99.2
Generously allowed (%)	0.8
Disallowed (%)	0.0

mm, main chain–main chain; ms, main chain–side chain; ss, side chain–side chain. *Root-mean-squared deviation (rmsd) from ideal bond lengths and angles and rmsd in B-factors of bonded atoms.

the Oγ atom of Thr-149 and the N atom of Val-149c (3.02 Å), and N atom of Thr-149 and the O atom of Val-149c (2.78 Å). Further downstream from the second Pro ring, the methyl group of H-D-Ala is free of contacts, but the terminal *p*-methyl substituted Phe ring engages the aryl binding site of thrombin composed of Ile-174, Trp-215, and Leu-99 in extensive van der Waals interactions. These interactions are similar to those seen between the aryl binding site and the P3 H-D-Phe residue of the active site inhibitor PPACK [12,19]. The interaction is unique over previous versions (e.g. RPPGF) and surely contributes to the added potency of the compound. However, the Oic side chain interacts with the 60-loop of thrombin in a way that resembles the P2 Pro residue of PPACK [12,19]. In summary, the interaction of FM19 with thrombin is driven mainly by polar contacts of the H-D-Arg residue with the primary specificity pocket, hydrophobic interactions of the P2 Oic and *p*-methyl substituted Phe with the 60-loop and the aryl binding site, respectively. Additional strength to the binding interaction comes from water-mediated contacts with the 216–219 β-strand of the enzyme.

In vivo *investigations*

Initial investigations determined the pharmacokinetic profile of FM19. In purpose-bred beagle dogs, FM19 had a $t_{1/2}\alpha$ of

Table 5 Pharmacokinetic profile of FM19

	AUC [(mg l^{-1}) × min]	V_d (mL kg^{-1})	$t_{1/2\alpha}$ (min)	Clearance (mL min^{-1} kg^{-1})
Dog 1	330	5700	35	13
Dog 2	420	4900	30	12
Dog 3	960	2100	30	4.8
Dog 4	1500	1800	35	2.8
Mean ± SD	803 ± 542	3625 ± 1965	33 ± 2.9	8.2 ± 5.1

32.5 ± 2.9 min (mean ± SD) with a plasma clearance of 8.2 ± 5.1 mL min^{-1} kg^{-1} (Table 5). Similar investigations in the conscious Sprague–Dawley rat showed a $t_{1/2}\alpha$ of 27 ± 7 min with a plasma clearance of 10.9 ± 7 mL^{-1} min^{-1} kg^{-1}. FM19 is not metabolized *in vivo*. In pooled liver microsomes, no significant metabolism (< 20%) was observed after 120 min at 1 and 10 μM concentrations with 1 mg mL^{-1} microsomal protein.

Investigations next determined the influence of FM19 on carotid artery thrombosis induced by free radical injury after laser light on intravascular Rose Bengal. In C57BL/6j mice, FM19 at ≥0.2 mg kg^{-1} IP significantly prolonged the time to carotid artery thrombosis from 32 ± 2.5 min (untreated) to 38 ± 2.2 min ($P = 0.04$) or longer at higher concentrations of added peptide (Fig. 6A).

Because FM19 does not contain a peptide bond between two natural amino acids, studies determined it was stable in rat intestinal juices (data not shown). Investigations next determined if FM19 would be taken up in the intestine when instilled into the duodenum. Instillation of 32 mg kg^{-1} FM19 in 100 μL in the duodenum of B6129 mice resulted in a plasma concentration of 1.53 μg mL^{-1} at 1 h as determined by LC/MS/MS assay. Instillation of FM19 in the duodenum at 8.25, 16, or 33 mg kg^{-1} in B6129 mice resulted in a significant prolongation ($P < 0.0034$) of the time of carotid artery occlusion from 22 ± 2 min (control) (mean ± SEM) to 38 ± 4 min and 62 ± 8 min and in the 16 and 33 mg kg^{-1} FM19-treated mice, respectively (Fig. 6B). Furthermore, the TCT in mice treated with 33 mg kg^{-1} in the duodenum significantly increased from 21 s at baseline to 29 s at 30 min, 37 s at 1 h, and 50 s at 2 h ($P \leq 0.01$). The APTT and PT under the same conditions were significantly prolonged at 2 h ($P < 0.019$) (data not shown).

Studies next determined if FM19 was effective after oral administration. FM19 (3, 5 or 10 mg mL^{-1}) was added to the drinking water of B6129 mice for 7–10 days and the animals were examined in the Rose Bengal carotid artery thrombosis model (Fig. 6C). FM19 at 5 mg mL^{-1} or greater significantly prolonged the time to thrombosis to 62 ± 7.1 min from 23 ± 1.1 min for untreated animals ($P = 0.002$). Further, the TCT was prolonged from 24.3 ± 1.8 s in untreated mice to 175 ± 14 s (mean ± SD) with treatment. The murine plasma level of orally administered FM19 after seven or more days was 80 ± 9, 173 ± 16, or 244 ± 135 ng mL^{-1} (mean ± SD) for 3, 5, or 10 mg mL^{-1} in drinking water, respectively. Further studies showed that just two days of 5 mg mL^{-1} FM19 in the drinking water prolonged the time to thrombosis in these animals to 46 ± 5 min with a TCT to 43 ± 3 s and a plasma concentration of 128 ± 28 ng mL^{-1}. These combined data indicated that FM19 is orally active as a direct thrombin inhibitor.

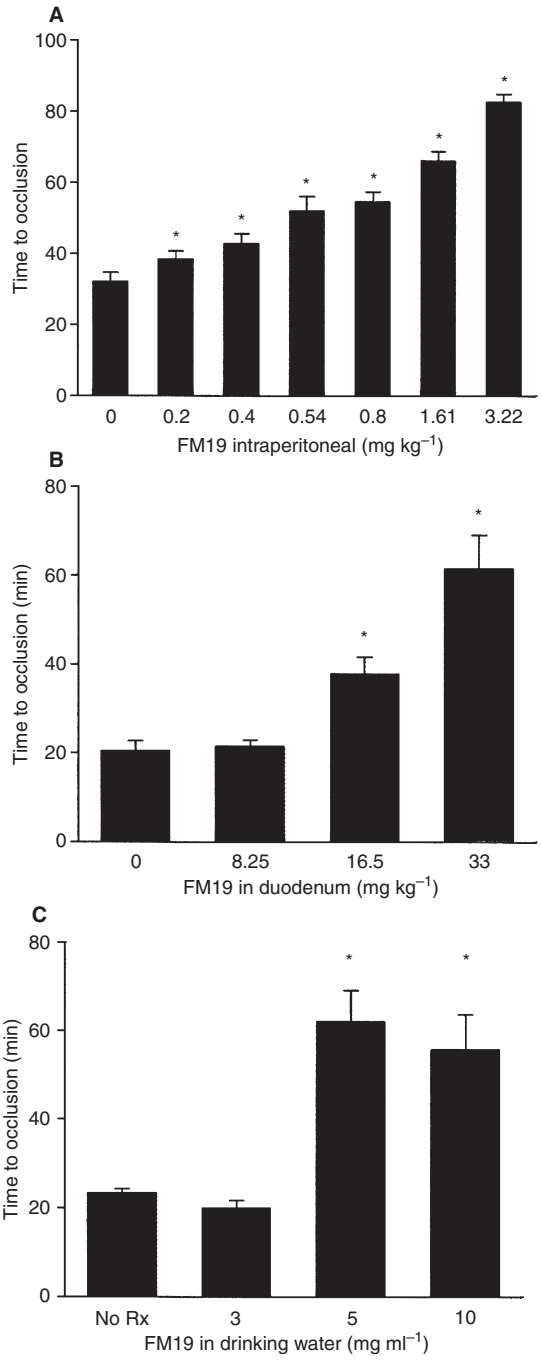

Fig. 6. Influence of FM19 on mouse carotid artery thrombosis initiated by photooxidation of Rose Bengal. C57Bl/6j mice were prepared for Rose Bengal studies to determine the time thrombosis in the absence or presence of 0.2–3.22 mg kg^{-1} FM19 intraperitoneal injection (A). B6:129SF2/j mice were prepared for Rose Bengal studies to determine the time thrombosis in the absence or presence of 8.25–33 mg kg^{-1} FM19 injected into the duodenum (B) or 3–10 mg mL^{-1} FM19 in the drinking water (C). The data are the mean ± SD of at least three or more experiments.

Discussion

Previous studies demonstrate that the angiotensin-converting enzyme (ACE) breakdown product, RPPGF, inhibits thrombin-mediated platelet aggregation in man and the time to thrombosis in animal models [5–7,9]. Currently, we improved the potency and stability of these compounds by substituting D-isomers and/or unusual amino acids at residues 4 or 5 of the previous lead compound, TH146 (rOicPGF) (Table 1) [7,10]. Five initial compounds inhibited threshold γ-thrombin induced platelet aggregation 4- to 9-fold better than TH146. Of these, FM19 [rOicPaF(*p*-Me)] was chosen for further study. FM19 completely inhibited platelet aggregation at concentrations 9-fold lower than TH146 and forty-threefold lower than RPPGF (Table 1). FM19 was also a nineteenfold better inhibitor of α-thrombin-induced calcium mobilization in human fibroblast (IC_{50} = 6.9 μM for FM19 vs. 130 μM for TH146) and has a twenty-twofold lower K_i (4.4 μM for FM19 vs. 97 μM for TH146). These data demonstrate that changes at residues 4 and 5 result in a peptide that is ~twentyfold more potent than the previous lead compound. The improved potency of FM19 over TH146 is most likely attributed to the physical interaction of the P5 *p*-methyl-substituted Phe ring of the C-terminal residue with thrombin.

Kinetic analysis, X-ray crystallography and *in vitro* clotting assays demonstrate that FM19, like previous iterations of RPPGF derivates, interacts directly with thrombin. FM19 is a competitive inhibitor (K_i = 4.4 μM; Fig. 4, Table 3) of thrombin cleavage of a chromogenic substrate (S2238). This assessment is supported by direct crystallographic evidence that FM19 binds to the active site of thrombin in a retro-binding orientation (Fig. 5). This interaction is largely mediated by its first residue D-Arg. The structure of thrombin in complex with the naturally occurring peptide, RPPGF, also showed the N-terminal Arg interacting with the S1 pocket in a retro-binding orientation [6]. In peptides where the N-terminal Arg is removed, there is no inhibitory activity (Table 1). In contrast to RPPGF, the second position of FM19, Oic, interacts with the 60-loop (Tyr60a and Trp60d) moving the indole ring of Trp60d >4 Å. Further, the Phe at residue 5 of RPPGF was not resolved from the density map in the thrombin complex [6]. In contrast, residue 5 of FM19 makes well-defined hydrophobic contacts with the aryl binding pocket of thrombin, which is important for thrombin's interaction with polypeptide substrates [12,19]. These interactions likely contribute to the ~four hundredfold decrease in the K_i of FM19 vs. RPPGF (Fig. 4, Table 3) and the ~one hundred and sixtyfold decrease in the minimal concentration required to prolong *in vitro* thrombin clotting time (Fig. 3, Table 2) [6].

In addition to directly interacting with thrombin, previous iterations of this group of compounds appeared to bind to the exodomains of PAR1 and PAR4 at the thrombin cleavage sites, preventing activation of these receptors [6–8]. Modification of residues 4 and/or 5 of TH146 resulted in loss of this activity while increasing its direct thrombin inhibition. FM19 was unable to consistently and specifically bind to recombinant PAR1 or PAR4 exodomain in *in vitro* binding assays (data not shown). Further, FM19 was unable to inhibit PAR1 or PAR4 activation by plasmin- or cathepsin G-induced Ca^{2+} mobilization on HeLa cells transfected to express PAR1 or PAR4 (data not shown) [20,21]. It is possible FM19 binds to PAR1 and 4 such that it cannot block plasmin or cathepsin G proteolysis of the exodomain. However, it is more likely that the substitutions made at residues 4 and/or 5 alter the structure of FM19 such that it improves its direct thrombin inhibition at the expense of its binding to PAR1 and PAR4.

Although the Thrombostatin FM compounds have lost their ability to bind to PAR1 and PAR4, they represent an improvement over previous iterations of these compounds [7,22]. First, they are more potent in all assays [7,22]. Secondly, as these compounds have no peptide bonds between two L-amino acids, they are stable in biologic fluids allowing for oral delivery. When animals were given ≥5 mg kg^{-1} FM19 orally for two to seven days, the plasma levels of FM19 (128–244 ng mL^{-1}) were increased sufficiently to prevent arterial thrombosis. Thirdly, the mechanism of action of the Thrombostatin FM compounds may make them more apt to inhibit platelet thrombin receptor activation than other direct thrombin inhibitors. The fact that the N-terminal H-D-Arg fills the S1 pocket of the active site of thrombin may be particularly effective to prevent PAR1 or PAR4 binding and activation. Such a mechanism of inhibition may have improved inhibition of platelet activation over more potent direct thrombin inhibitors, such as hirudin or bivalirudin, which have to also interact with thrombin's exosite 1. Further, the potency and irreversibility of an agent such as hirudin also increases bleeding risk, which alone reduces overall clinical outcomes [4,23]. Previous studies have shown that cleaved PAR3 on murine platelets binds to thrombin's exosite 1 to open thrombin's S1 pocket to facilitate PAR4 activation [24]. If a similar mechanism occurs between cleaved PAR1 and PAR4 on human platelets, FM19-like compounds may prove to be better direct thrombin inhibitors to prevent platelet activation.

Addendum

The contributions of each of the authors was as follows: Drs Burke, Mosberg, and Schmaier created the compounds; Mr Warnock, Ms Zhou, Dr Burke, and Dr Andrew Chen performed inhibition of platelet aggregations studies; Mr Warnock, Dr Burke, Dr Andrew Chen, and Dr Nieman performed inhibition of calcium flux; Mr Warnock, Ms Zhou, Mr Sweigart, and Dr Burke performed the coagulation studies; Mr Warnock, Mr Sweigart, Dr Burke, and Dr Nieman performed the enzymatic inhibition studies; Mr Ricketts, Mr Sweigart, and Dr Burke performed the peptide–protein binding studies; Drs Zhiwei Chen and Di Cera performed the crystallography; Mr Warnock and Drs Lucchesi and Schmaier performed the pharmacokinetic studies in dogs and rats; Drs Hilfinger and Kim developed the LC/MS/MS assay and with Dr Schmaier created the studies for the oral administration; Mr Warnock and Ms Zhou performed the murine thrombosis studies. All authors contributed to the preparation of the

manuscript, but major sections were written by Drs Nieman, Di Cera, and Schmaier.

Acknowledgements

This work was supported in part by the National Institutes of Health Research Grants HL52779 and HL55709 (to A. H. Schmaier), HL86038 (to J. Hilfinger, H. I. Mosberg, and A. H. Schmaier), and HL49413, HL58141 and HL73813 (to E. Di Cera).

Disclosure of Conflict of Interests

The authors state that they have no conflict of interest. J. Hilfinger and A. H. Schmaier have conflict of interest as stockholders and Officers of companies that may commercialize this technology. The other authors state that they have no conflict of interest.

Supplementary material

The following supplementary material can be found at http://www.blackwell-synergy.com/loi/jth:

Sample preparation, LC/MS/MS analysis, and metabolic stability and *in vitro* half-life of FM19 in human, canine and rat liver microsomes.

This material is available as part of the online article from http://www.blackwell-synergy.com/doi/abs/10.1111/j.1538-7836.2008.02937.x (This link will take you to the article abstract).

Please note: Blackwell Publishing are not responsible for the content or functionality of any supplementary materials supplied by the authors. Any queries (other than missing material) should be directed to the corresponding author for the article.

References

1 Yusuf S, Zhao F, Mehta SR, Chrolavicius S, Tognoni G, Fox KK. Effects of clopidogrel in addition to aspirin in patients with acute coronary syndromes without ST-segment elevation. *N Engl J Med* 2001; **345**: 494–502.

2 Matetzky S, Shenkman B, Guetta V, Shechter M, Bienart R, Goldenberg I, Novikov I, Ores H, Savion N, Varon D, Hod H. Clopidogrel resistance is associated with increased risk of recurrent atherothrombotic events in patients with acute myocardial infarction. *Circulation* 2004; **109**: 3171–5.

3 Angiolillo DJ, Bernardo E, Sabate M, Jimenez-Quevedo P, Costa MA, Palazuelos J, Hernandez-Antolin R, Moreno R, Escaned J, Alfonso F, Banuelos C, Guzman LA, Bass TA, Macaya C, Fernandez-Ortiz A. Impact of platelet reactivity on cardiovascular outcomes in patients with type 2 diabetes mellitus and coronary artery disease. *J Am Coll Cardiol* 2007; **50**: 1541–8.

4 Wiviott SD, Braunwald E, McCabe CH, Montalescot G, Ruzyllo W, Gottlieb S, Neumann F-J, Ardissino D, De Servi S, Murphy SA, Riesmeyer J, Weerakkody G, Gibson CM, Antman EM for the TRITON-TIMI 38 Investigators. Prasugrel versus clopidogrel in patients with acute coronary syndromes. *N Engl J Med* 2007; **357**: 2001–15.

5 Hasan AA, Amenta S, Schmaier AH. Bradykinin and its metabolite, Arg-Pro-Pro-Gly-Phe, are selective inhibitors of alpha-thrombin-induced platelet activation. *Circulation* 1996; **94**: 517–28.

6 Hasan AA, Warnock M, Nieman M, Srikanth S, Mahdi F, Krishnan R, Tulinsky A, Schmaier AH. Mechanisms of Arg-Pro-Pro-Gly-Phe inhibition of thrombin. *Am J Physiol Heart Circ Physiol* 2003; **285**: H183–93.

7 Nieman MT, Warnock M, Hasan AA, Mahdi F, Lucchesi BR, Brown NJ, Murphey LJ, Schmaier AH. The preparation and characterization of novel peptide antagonists to thrombin and factor VIIa and activation of protease-activated receptor 1. *J Pharmacol Exp Ther* 2004; **311**: 492–501.

8 Nieman MT, Pagan-Ramos E, Warnock M, Krijanovski Y, Hasan AA, Schmaier AH. Mapping the interaction of bradykinin 1-5 with the exodomain of human protease activated receptor 4. *FEBS Lett* 2005; **579**: 25–9.

9 Murphey LJ, Malave HA, Petro J, Biaggioni I, Byrne DW, Vaughan DE, Luther JM, Pretorius M, Brown NJ. Bradykinin and its metaboliste bradykinin 1-5 inhibit thrombin-induced platelet aggregation in humans. *J Pharmacol Exp Ther* 2006; **318**: 128701292.

10 Burke FM, Warnock M, Schmaier AH, Mosberg HI. Synthesis of novel peptide inhibitors of thrombin-induced platelet activation. *Chem Biol Drug Des* 2006; **68**: 235–8.

11 Nieman MT, Schmaier AH. Interaction of thrombin with PAR1 and PAR4 at the thrombin cleavage site. *Biochemistry* 2007; **46**: 8603–10.

12 Pineda AO, Carrell CJ, Bush LA, Prasad S, Caccia S, Chen ZW, Mathews FS, Di Cera E. Molecular dissection of Na+ binding to thrombin. *J Biol Chem* 2004; **279**: 31842–53.

13 Otwinowski Z, Minor W. Processing of X-ray diffractin data collected in oscillation mode. *Methods Enzymol* 1997; **276**: 307–26.

14 Bailey S. The CCP4 Suite: programs for protein crystallography. *Acta Crystallogr D Biol Crystallogr* 1994; **50**: 760–3.

15 Brunger AT, Adams PD, Clore GM, DeLano WL, Gros P, Grosse-Kunstleve RW, Jiang JS, Kuszewski J, Nilges M, Pannu NS, Raed RJ, Rice LM, Simonson T, Warren GL. Crystallography & NMR system: a new software suite for macromolecular structure determination. *Acta Crystallogr D Biol Crystallogr* 1998; **54**: 905–21.

16 Morris AL, MacArthur MW, Hutchinson EG, Thornton JM. Stereochemical quality of protein structure coordinates. *Proteins* 1992; **12**: 345–64.

17 Rowland M, Tozer T. *Clinical Pharmacokinetics Concepts and Application*, 2nd edn. Philadelphia, PA: Lea and Febiger, 1989.

18 Cleary DB, Ehringer WD, Maurer MC. Establishing the inhibitory effects of bradykinin on thrombin. *Arch Biochem Biophys* 2003; **410**: 96–106.

19 Bode W, Turk D, Karshikov A. The refined 1.9-A X-ray crystal structure of D-Phe-Pro-Arg chloromethylketone-inhibited human alpha-thrombin: structure analysis, overall structure, electrostatic properties, detailed active-site geometry, and structure-function relationships. *Protein Sci* 1992; **1**: 426–71.

20 Kuliopulos A, Covic L, Seeley SK, Sheridan PJ, Helin J, Costello CE. Plasmin desensitization of the PAR1 thrombin receptor: kinetics, sites of truncation, and implications for thrombolytic therapy. *Biochemistry* 1999; **38**: 4572–85.

21 Sambrano GR, Huang W, Faruqi T, Mahrus S, Craik C, Coughlin SR. Cathepsin G activates protease-activated receptor-4 in human platelets. *J Biol Chem* 2000; **275**: 6819–23.

22 Hasan AA, Warnock M, Srikanth S, Schmaier AH. Developing peptide inhibitors to thrombin activation of platelets from bradykinin analogs. *Thromb Res* 2001; **104**: 451–65.

23 Antman EM, Hirudin in acute myocardial infarction. Safety report from the thrombolysis and thrombin inhibition in myocardial infarction (TIMI) 9A trial. *Circulation* 1994; **90**: 1624–30.

24 Bah A, Chen Z, Bush-Pelc LA, Mathews FS, Di Cera E. Crystal structures of murine thrombin in complex with the extracellular fragments of murine protease-activated receptors PAR3 and PAR4. *Proc Natl Acad Sci USA* 2007; **104**: 11603–8.